

The SOLAS Air-Sea Gas Exchange Experiment (SAGE) 2004.

Mike J. Harvey¹, Cliff S. Law¹, Murray J. Smith¹, Julie A. Hall², Edward R. Abraham^{1,A}, Craig L. Stevens¹, Mark G. Hadfield¹, David T. Ho^{3,B}, Brian Ward^{4,C}, Stephen D. Archer⁵, Jill M. Caine⁶, Kim I. Currie⁷, Dawn Devries⁸, Michael J. Ellwood^{2,D}, Peter Hill¹, Graham B. Jones⁹, Dave Katz^{10#}, Jorma Kuparinen¹¹, Burns Macaskill^{2#}, William Main^{1#}, Andrew Marriner¹, John McGregor¹, Craig McNeil¹⁰, Peter J. Minnett¹², Scott D. Nodder¹, Jill Peloquin¹³, Stuart Pickmere², Matthew H. Pinkerton¹, Karl A. Safi², Rona Thompson^{1#}, Matthew Walkington¹, Simon W. Wright¹⁴, Lori A. Ziolkowski^{15#}

¹National Institute of Water and Atmospheric Research (NIWA), P.O. Box 14-901, Kilbirnie, Wellington, New Zealand

²National Institute of Water and Atmospheric Research (NIWA), P.O. Box 11-115, Hamilton, New Zealand

³Lamont-Doherty Earth Observatory of Columbia University, 61 Route 9W Palisades, NY 7 10964, U.S.A.

⁴Woods Hole Oceanographic Institution, 266 Woods Hole Road, Woods Hole, MA 02543-1050, U.S.A.

⁵Plymouth Marine Laboratory, Prospect Place, West Hoe, Plymouth, PL1 3DH, U.K.

⁶Cape Grim B.A.P.S., Bureau of Meteorology, PO Box 346, Smithton, Tasmania 7330 Australia

⁷National Institute of Water and Atmospheric Research (NIWA), Centre for Chemical and Physical Oceanography, Department of Chemistry, University of Otago, Dunedin, New Zealand

⁸University of Colorado Denver, P.O. Box 173364, Denver, Colorado 80217-3364, U.S.A.

⁹Centre for Climate Change Studies, School of Environmental Science and Management, Southern Cross University, Lismore, NSW 2480, AUSTRALIA

¹⁰Graduate School of Oceanography, University of Rhode Island, South Ferry Road, Narragansett, RI 02882 USA

¹¹Department of Biological and Environmental Sciences, P.O. Box 65, FI-00014 University of Helsinki, Finland

¹²Meteorology & Physical Oceanography, Rosenstiel School of Marine & Atmospheric Science, University of Miami, 4600 Rickenbacker Causeway, Miami, FL 33149-109, USA

¹³Virginia Institute of Marine Science, College of William and Mary, P.O. Box 1346, Gloucester Point, VA 23062. U.S.A.

¹⁴Australian Antarctic Division, Channel Highway, Kingston, Tasmania 7050, Australia

¹⁵Department of Oceanography, Dalhousie University, Halifax, NS B3H 4J1, Canada

#No longer affiliated with organisation

Current Affiliation:

^ADragonFly, Wellington, New Zealand.

^BDepartment of Oceanography, University of Hawaii, 1000 Pope Road, MSB 517, Honolulu, HI 96822, USA

^CSchool of Physics & Environmental Change Institute, National University of Ireland, University Road, Galway, Ireland

^DDepartment of Earth and Marine Sciences, Australian National University, Canberra, Australia

Keywords: air-sea gas exchange, iron fertilisation, ocean biogeochemistry, SOLAS

1 Abstract

2 The SOLAS air-sea gas exchange experiment (SAGE) was a multiple-objective study investigating
3 gas-transfer processes and the influence of iron fertilisation on biologically driven gas exchange in
4 high-nitrate low-silicic acid low-chlorophyll (HNLSiLC) Sub-Antarctic waters characteristic of the
5 expansive Subpolar Zone of the southern oceans. This paper provides a general introduction and
6 summary of the main experimental findings. The release site was selected from a pre-voyage desktop
7 study of environmental parameters to be in the south-west Bounty Trough (46.5°S 172.5°E) to the
8 south-east of New Zealand and the experiment conducted between mid-March and mid-April 2004. In

9 common with other mesoscale iron addition experiments (FeAX's), SAGE was designed as a
10 Lagrangian study quantifying key biological and physical drivers influencing the air-sea gas exchange
11 processes of CO₂, DMS and other biogenic gases associated with an iron-induced phytoplankton
12 bloom. A dual tracer SF₆/³He release enabled quantification of both the lateral evolution of a labelled
13 volume (patch) of ocean and the air-sea tracer exchange at the 10's of km's scale, in conjunction with
14 the iron fertilisation. Estimates from the dual-tracer experiment found a quadratic dependency of the
15 gas exchange coefficient on windspeed that is widely applicable and describes air-sea gas exchange in
16 strong wind regimes. Within the patch, local and micrometeorological gas exchange process studies
17 (100 m scale) and physical variables such as near-surface turbulence, temperature microstructure at the
18 interface, wave properties, and wind speed were quantified to further assist the development of gas
19 exchange models for high-wind environments.

20
21 There was a significant increase in the photosynthetic competence (F_v/F_m) of resident phytoplankton
22 within the first day following iron addition, but in contrast to other FeAX's, rates of net primary
23 production and column-integrated chlorophyll *a* concentrations had only doubled relative to the
24 unfertilised surrounding waters by the end of the experiment. After 15 days and four iron additions
25 totalling 1.1 tonne Fe²⁺, this was a very modest response compared to the other mesoscale iron
26 enrichment experiments. An investigation of the factors limiting bloom development considered co-
27 limitation by light and other nutrients, the phytoplankton seed-stock and grazing regulation. Whilst
28 incident light levels and the initial Si:N ratio were the lowest recorded in all FeAX's to date, there was
29 only a small seed-stock of diatoms (less than 1% of biomass) and the main response to iron addition
30 was by the picophytoplankton. A high rate of dilution of the fertilised patch relative to phytoplankton
31 growth rate, the greater than expected depth of the surface mixed layer and microzooplankton grazing
32 were all considered as factors that prevented significant biomass accumulation. In line with the limited
33 response, the enhanced biological draw-down of pCO₂ was small and masked by a general increase in
34 pCO₂ due to mixing with higher pCO₂ waters. The DMS precursor DMSP was kept in check through
35 grazing activity and in contrast to most FeAX's dissolved dimethylsulfide (DMS) concentration
36 declined through the experiment. SAGE is an important low-end member in the range of responses to
37 iron addition in FeAX's. In the context of iron fertilisation as a geoengineering tool for atmospheric
38 CO₂ removal, SAGE has clearly demonstrated that a significant proportion of the low iron ocean may
39 not produce a phytoplankton bloom in response to iron addition.

40

41 **Introduction**

42 Of the $\sim 8 \text{ Pg yr}^{-1}$ of carbon emitted to the atmosphere through fossil fuel combustion
43 (Canadell et al., 2007), there is a net annual uptake of $\sim 5 \text{ PgC yr}^{-1}$ split roughly equally
44 between terrestrial and ocean sinks. Within the latitude band from 40° to 60°S there exists a
45 strong sink region associated with photosynthetic (biological) carbon uptake, and Takahashi
46 *et al.* (2009) have identified the southern hemisphere oceans (south of 14°S to Antarctica) as
47 providing the largest oceanic sink region for CO_2 . Increased observation has helped to refine
48 this estimate. Takahashi *et al.* (2002) previously identified a disproportionate influence of the
49 southern oceans (between 50 and 62°S), which occupy 10% of the global ocean yet account
50 for 20% of the global CO_2 uptake, although the more recent estimates by Takahashi *et al.*
51 (2009) with a 3x larger database do not support such a large influence. This net uptake of
52 CO_2 reflects the balance between the biological drawdown during summer and significant
53 emission in winter.

54
55 There is uncertainty in the mean ocean uptake of CO_2 , and its inter-annual variability, due in
56 part to windspeed dependence of the gas exchange coefficient k (Carr et al., 2002; Olsen et
57 al., 2005). There are a number of wind-based parameterisations of k derived from
58 observation: Liss and Melivat (1986) found a linear-spline relationship to wind; Wanninkhof
59 (1992) and Nightingale *et al.* (2000) a quadratic relationship; Wanninkhof *et al.* (2004) either
60 quadratic or cubic and Wanninkhof and McGillis (1999) a cubic relationship. Clearly
61 estimates from these different parameterisations will diverge with increase in windspeed and
62 so the uncertainty in k will be larger at higher windspeed. The requirement to further
63 constrain the processes determining gas-exchange is especially relevant to the subantarctic
64 waters where zonally averaged windspeeds increase poleward through the mid-latitude 40° to
65 60°S storm belt (Sura, 2003). Processes associated with strong winds, such as bubble-
66 mediated exchange (D'Asaro and McNeil, 2008; Woolf, 1997), will not be adequately
67 accounted for in parameterisations developed at lower windspeed. In addition to the wind
68 influence on the magnitude of surface air-sea exchange processes, concern has arisen from
69 model analyses that suggest the CO_2 sink strength in this region could in fact decline due to
70 the poleward displacement and intensification of westerly winds that drive increased
71 upwelling of carbon rich waters from the ocean interior (Le Quéré et al., 2007). The certainty
72 of this finding is still the subject of debate, in part because the model predictions are poorly
73 constrained by observation (Law et al., 2008). Model results presented by Zickfeld (2008)
74 found that as atmospheric CO_2 continues to rise through the 21st century, the efficiency of the
75 southern ocean sink will tend to increase.

76

77

78 This paper provides a general introduction and summary of the main experimental findings of
79 the SOLAS Air-Sea Gas Exchange Experiment (SAGE). Accompanying papers in this
80 volume provide more details of the results of SAGE conducted in sub-Antarctic waters of the
81 south-west Bounty Trough (46.5°S 172.5°E) between mid-March and mid-April 2004. The
82 experiment used the $^3\text{He}/\text{SF}_6$ dual tracer method which has been successfully used in the open
83 ocean to provide a patch-scale (10-100 km) air-sea gas exchange estimate in a diffusive ocean
84 mixed-layer (Nightingale et al., 2000; Wanninkhof, 1993; Wanninkhof et al., 1997;
85 Wanninkhof et al., 2004). Whilst most of the existing dual tracer gas exchange data from
86 ocean experiments are from shallower water bodies such as the North Sea, Georges Bank, or
87 the Florida Shelf, these studies have confirmed that the uncertainty in the parameterization of
88 gas exchange coefficient k increases as a function of wind speed, and so refinement of the
89 parameterisation is particularly important in regions such as the subantarctic waters which are
90 subject to high wind speeds. For SAGE, the dual-tracer release was complemented by
91 micrometeorological-scale gas exchange determination and measurement of the dominant
92 physical processes known to affect gas exchange, including wind speed, near surface
93 turbulence, the micro-structure of temperature and salinity, and wave characteristics.

94

95 From early planning stages, SAGE was devised as a combined gas-exchange process and
96 mesoscale iron fertilisation experiment. The initial aim was to produce a purposefully
97 stimulated and tracer labelled phytoplankton bloom, and provide a laboratory in the natural
98 environment for study of enhanced biogeochemical fluxes and associated air-sea gas
99 exchange, particularly of CO_2 and DMS driven by the biological activity. The southern
100 oceans are the largest High Nutrient Low Chlorophyll (HNLC) area of ocean where
101 productivity is limited by levels of the micro-nutrient iron. Previous experience with iron
102 fertilisation has shown that significant enhancement of algal biomass and primary production
103 can occur (e.g. Boyd et al., 2000; Trull et al., 2001). The results of a review of eight
104 mesoscale fertilisations (de Baar et al., 2005) has since confirmed that maximum biological
105 signal typically scales inversely with the depth of the wind-mixed layer, mediated through the
106 relationship between underwater light climate and phytoplankton photosynthesis.

107

108 The HNLC condition as applied to sub-Antarctic waters is more precisely described as
109 (HNLSiLC) or “low-silicic acid HNLC” (Dugdale and Wilkerson, 1998). This condition is
110 found over much of the southern hemisphere oceans in the Sub-Antarctic zone south of 45°S
111 down to the Antarctic Polar frontal zone (Brzezinski et al., 2005). This HNLSiLC ocean area
112 south of 45°S is approximately twice that of HNLC polar waters south of 60°S. Following
113 addition of iron to the low Si waters, it is highly likely that silicic acid will rapidly limit the

114 development of diatoms (Coale et al., 2004). Prior to SAGE, there was interest in examining
115 the response to iron over a longer duration into the bloom decline phase, as done with the
116 European Iron Fertilisation Experiment EIFEX (Bathmann, 2005), with the aim of
117 quantifying carbon sedimentation fluxes. Following the SAGE experiment, there has been
118 further synthesis of the results from 12 mesoscale iron addition experiments including SAGE
119 (Boyd et al., 2007) and heightened interest in the prospects of ocean (iron) fertilisation as a
120 (bio)geoengineering solution to atmospheric CO₂ build-up (Lenton and Vaughan, 2009).
121 However, the need for caution has been clearly identified due to the relatively low efficiency
122 as a carbon sink (Boyd et al., 2004), the difficulty in confirming the degree of permanence of
123 CO₂ removal from the atmosphere and the large uncertainty around unplanned consequences
124 and other environmental impacts without further biogeochemical research (Buesseler and
125 Boyd, 2003; Buesseler et al., 2008).

126

127 The progression in iron fertilisation experimentation from incubation study (Martin et al.,
128 1990), to open-ocean equatorial HNLC (Coale et al., 1996), to the Southern Ocean HNLC
129 (Boyd et al., 2000), and more recently to longer-term tracking (Coale et al., 2004), and natural
130 fertilisation study (Blain et al., 2001; Pollard et al., 2009), has been mirrored to an extent by
131 advances in gas exchange studies. Early wind tunnel experiments (Liss, 1983) have been
132 followed by shelf-sea tracer experiments (Nightingale et al., 2000; Wanninkhof et al., 1997) to
133 open ocean process studies (Fairall et al., 2000; Feely et al., 2004; Ward et al., 2004). More
134 recently, attention turned to the higher windspeed regime of the southern oceans (Wanninkhof
135 et al., 2004) where there has been little in-situ study, given the logistic challenges of this
136 work. In extending the observational work at the time, there is no doubt that the combined
137 broad goals of mesoscale iron fertilisation and gas-exchange process study under episodic
138 high-wind conditions, as proposed by SAGE, were ambitious.

139

140 **Experimental goals and site selection**

141 SAGE had three main experimental goals to determine the drivers and controls of ocean-
142 atmosphere gas exchange through quantification of:

- 143 ■ *biological production and utilisation of climatic relevant gases (in particular CO₂ and*
144 *DMS) in the surface ocean in association with a phytoplankton bloom through*
145 *measurement of environment and ecosystem variables, dissolved and atmospheric gas*
146 *concentrations;*
- 147 ■ *physical control of gas exchange across the interfaces of the surface mixed layer through*
148 *the dual tracer method at the patch scale (Ho et al., 2006), ship-borne*
149 *micrometeorological flux measurement, with a combination of in-situ measurement of*
150 *boundary layer exchange and remote sensing of the air-sea interface for sea surface*
151 *temperature and wave properties;*

152 ▪ *production of aerosols resulting from interaction of biological and physical processes, (in*
153 *particular, study of the oxidation products of DMS) through measurement of the*
154 *atmospheric mixing ratios of DMS, SO₂ and condensation nuclei properties.*
155

156 There were five criteria that guided the site selection:

- 157 1. a relatively quiescent and homogeneous region allowing tracer labelled patch tracking
158 for up to a month.
- 159 2. a 30 to 80 m mixed layer depth to limit dilution of SF₆ and iron
- 160 3. a range of atmospheric wind speeds to allow study of gas exchange coefficient—wind
161 speed relationship
- 162 4. Non-limiting macro-nutrient availability and phytoplankton in HNLC waters
163 receptive to iron fertilisation
- 164 5. low variability and shear in currents on the patch scale for maintenance of a coherent
165 patch.

166
167 Sites for SAGE were identified in a pre-experiment desktop study (Hadfield, 2010) at three
168 potential locations. Site 1 at the NIWA Southern Biophysical time series mooring (S. Bio
169 Mooring in Figure 1) 46° 40'S, 178° 30'E, was rejected as possibly too dynamic, as was found
170 with the FeCycle experiment conducted at this location (Boyd et al., 2005). The second site
171 on the Central Campbell Plateau, approximately 169.5°E, 50.5°S, is relatively quiescent but
172 has consistently low phytoplankton stocks based on remote-sensing data. The third and
173 chosen site was around the South-western Bounty Trough, at approximately 47° 0'S, 172° 0'E
174 shown as the red dot in Figure 2. In this region of Sub-Antarctic waters, the mean flow is
175 towards the northwest, adjacent to the Southland Current and has lower current variability
176 than the SBM site. In common with the SBM site, the SAGE site has a naturally occurring
177 late summer (February) chlorophyll maximum (Figure 3) which in 2004 peaked at around
178 0.5 mg m⁻³ satellite-derived chlorophyll *a*. Examination of remote sensing data (SST, SSH
179 and ocean colour) immediately prior to the voyage lead to the decision to move the site
180 slightly east to avoid entrainment into the Southland current. Following the pre-release
181 survey, the first iron infusion was made at 46° 44'S 172° 32'E (Law et al., 2010).

182

183 In the following summary it is apparent that not all the site selection criteria were met,
184 particularly those related to “quiescence” and low current speed and sheer, and the
185 consequences of this are discussed.

186 **Initial conditions and iron addition**

187

188 Table 1 gives the initial upper ocean conditions at the time of the first infusion, made just east
189 of the cyclonic eddy centred at 47°S 172°E (Figure 4) which was a persistent feature during
190 SAGE. In Figure 5 the cruise track is overlaid on a geostrophic current plot. More detail on
191 the infusion pattern and subsequent evolution of the labelled patch are presented by Law *et al.*
192 (2010).

193

194 For the iron addition, a solution was prepared in two plastic 7500 litre tanks that were initially
195 half-filled with seawater and acidified to ~pH 2 by the addition of 25 litres of hydrochloric
196 acid. A total of 1.35 tonnes of $\text{FeSO}_4 \cdot 7\text{H}_2\text{O}$ (containing 274 kg Fe^{2+}) were used in each
197 infusion. The aim was to raise the initial dissolved iron concentration to 2nM over a 6x6 km
198 patch with a 50 m mixed layer depth. The dual tracer solution was prepared in two steel 4000
199 litre containers of seawater by saturation with SF_6 and ^3He . A headspace of ~5 L was
200 continuously flushed with SF_6 and circulated through the water via a diffusion hose by pump,
201 until the water was saturated. ^3He saturation was undertaken just prior to release, with ~10
202 litres of ^3He dissolved for 20 minutes of headspace recirculation (Law et al., 2010).

203

204 Details of the infusions are shown in Table 2 below. The iron and SF_6 solution were pumped
205 out at a depth of ~12-15m from a pipe attached to a towed fish at a distance of ~20m behind
206 the vessel. As sea-water was pumped out of the tracer tanks the volume was replaced by
207 water filling a meteorological balloon by gravity feed from the top of the tank; this flexible
208 cap minimised diffusive loss of ^3He and SF_6 that would have occurred if a headspace had
209 been allowed to develop. The 1st infusion on the 25 March covered 6 x 6 km and was
210 executed within a Lagrangian framework with an expanding hexagonal release track (with
211 track spacing of 0.7 km), referenced to a drogued drifter buoy at the nominal patch centre.
212 The need to reinfuse was dictated by the decline in SF_6 towards background concentrations.
213 The 2nd infusion on 31 March of iron, SF_6 and ^3He took place when the patch was distributed
214 as a long filament running NNW-SSE, and so was adapted to an along filament release track
215 of ~12 x 3 km using the nocturnal underway Fv/Fm signal as reference for patch location.
216 The 3rd infusion on 3 April was iron only, and was released using the underway surface SF_6
217 signal. The 4th and final infusion, of SF_6 and iron, on 6 April was released using the underway
218 Fv/Fm signal as reference because the dissolved SF_6 signal was low at this stage. All re-
219 infusions were successfully placed within the boundaries of the existing patch (Law et al.,
220 2010).

221 **Patch evolution and response to addition**

222 The accompanying papers in this volume expand on a number of key aspects of the SAGE
223 experiment. Unlike other experiments, there was no evidence for macro-nutrient depletion
224 during the experiment (Figure 6a) and there is a trend of nutrients increasing around days 5-8
225 when the fertilised area was affected by an interflow/intrusion of a water body at the west
226 boundary (Law et al., 2010). Whilst initial post-fertilisation dissolved iron levels were
227 generally greater than 1 nM (Table 2), values did decline rapidly although levels were
228 generally kept above 0.1-0.2 nM within the fertilised patch (Figure 6b). There was a rapid

229 initial response to iron addition detected as an increase in photosynthetic competence (F_v/F_m)
230 measured by fast repetition rate fluorometry (Figure 6d). The increase is consistent with
231 observations in other iron experiments (Boyd et al., 2000). A difference in F_v/F_m of ~ 0.04
232 between IN and OUT of the patch was maintained throughout the experiment based on the
233 threshold of 10 fM SF_6 as demarcation of the patch boundary (Law et al., 2010). After the
234 second infusion, this IN-OUT F_v/F_m difference was maintained against an increasing trend in
235 F_v/F_m outside the patch.

236

237 Kuparinen et al. (2010) identified that bacterioplankton growth rates were in general low with
238 no significant enhancement in the patch, but with the greatest increase towards the end of the
239 experiment. Phytoplankton stocks and primary productivity were slow to respond in spite of
240 the partial relief of iron stress with a small increase in surface chlorophyll *a* until Day 3
241 (Figure 6 c and e). Details are discussed by Peloquin *et al.* (2010b). Whilst a clear in-patch
242 enhancement in biomass and primary productivity appeared to exist around days 4-5, the
243 elevated IN concentrations declined the following day and there was then little difference
244 between IN and OUT patch values through to day 12 although the background values were
245 slowly increasing. From day 13 onwards, the in-patch chlorophyll *a* and IN-OUT difference
246 began once again to increase. The final enhancement (IN-OUT) at the end of the experiment
247 (day 16) was an approximate doubling of both surface (Figure 6 c and e) and column
248 integrated ($\sim 40 \text{ mg m}^{-2}$ OUT, $\sim 80 \text{ mg m}^{-2}$ IN) chlorophyll *a* and primary productivity
249 ($\sim 0.4 \text{ gC m}^{-2}\text{d}^{-1}$ OUT, $\sim 0.8 \text{ gC m}^{-2}\text{d}^{-1}$ IN) (Peloquin et al., 2010b). In the accompanying
250 volume we consider the component factors that are thought to have led to this modest
251 response (Law et al., 2010; Peloquin et al., 2010b).

252 **Limiting factors**

253 Physical factors limiting and causing the rapid shift in chlorophyll concentrations around days
254 5-6 were investigated. Figure 7 shows a summary of u_{10} wind statistics discussed in detail by
255 Smith *et al.* (2010). With the northward passage of a storm along the east coast of New
256 Zealand on day 3, there was an accompanying maximum in the recorded u_{10} windspeed of
257 $>20 \text{ m s}^{-1}$. The strong wind produced a deepening of the surface wind-mixed layer.
258 Comparison of the predicted conditions with those encountered by Hadfield (2010) identified
259 that the actual mixed-layer depth during SAGE was significantly greater than that predicted
260 by climatological values. Stevens *et al.* (2010) describe detailed physical measurements of the
261 ocean mixed-layer and environmental influences governing the mixed-layer depth and include
262 a new method for mixed-layer depth estimation. It was a few days after this storm around
263 days 5-8 that an interflow/intrusion produced a high rate of lateral dilution as the patch was
264 drifting north-east (Law et al., 2010). Chlorophyll concentrations did not increase further until

265 after the final infusion of iron, coincident with a decrease in windspeed and rate of patch
266 advection as well as improved meteorological conditions with higher incident light levels (*e.g.*
267 on days 9, 10, 12 in Figure 8). Law *et al.* (2010) found that there were only two periods when
268 the phytoplankton growth rate exceeded the minimum dilution rate (0.125 d^{-1}) on D3-6 and
269 D10-14, and these correspond to periods when IN station chlorophyll exceeded that at the
270 OUT station (Fig. 6c).

271

272 The pivotal role of light in limiting the development of diatom blooms in subantarctic waters
273 towards the equinox has been discussed by others (Boyd *et al.*, 1999; van Oijen *et al.*, 2004).
274 SAGE was conducted at a time and location that experienced the lowest range of theoretical
275 clear-sky photosynthetically active radiation (PAR) for any of the FeAX's (Figure 9). In the
276 figure we also show the likely range of surface PAR (allowing for cloud attenuation) using
277 the SeaWiFS PAR product described by Frouin (2003) for 8-day composite data of a 7×7 tile
278 of 9-km tile of pixels over the duration of each experiment. In these data, SAGE and
279 SOIREE have equal lowest median incident surface PAR. SOIREE was conducted in high
280 silicic acid polar waters (61°S) and there is a persistent trend of increasing fractional
281 cloudiness poleward from 30° to 60° (Mokhov and Schlesinger, 1994). In-situ measured PAR
282 data are available for both SOIREE and SAGE and there is good agreement with the median
283 of the in-situ and SeaWiFS estimates. The measured range for SOIREE was relatively large
284 between $13 - 40$ (average 21.4) $\text{mol m}^{-2} \text{ d}^{-1}$ and a significant bloom followed the alleviation of
285 iron stress (Boyd and Abraham, 2001). In SAGE, the range of PAR of $16 - 32$ (average 19.7)
286 $\text{mol m}^{-2} \text{ d}^{-1}$ was similar yet there was a much smaller biological response. Peloquin *et al.*
287 (2010a) consider in more detail macro- and micro-nutrients, light, seed-stocks and relative
288 rates of phytoplankton growth against grazing by micro- and meso-zooplankton and influence
289 of dilution of the patch. Peloquin *et al.* (2010a) suggest that received irradiance was not the
290 major limiting factor affecting the biological response of SAGE in the HNLSiLC waters
291 although the phytoplankton assemblage may have been on the cusp of light limitation.

292

293 The potential for macro-nutrient co-limitation was also assessed (Law *et al.*, 2010). The
294 mixed-layer deepening & intrusion resulted in an increase in mixed-layer macronutrient
295 concentrations until D10, with the result that concentrations were higher at end than the
296 beginning, unlike any other FeAX's. No significant floristic shifts occurred during the
297 experiment and, with a very low ($\sim 1\%$) initial diatom seed-stock in waters and the lowest
298 initial silicic acid to nitrate (Table 1) ratio of any of the iron addition experiments (Boyd *et al.*
299 *et al.*, 2007), there was little likelihood of a diatom bloom following the fertilisation. In the
300 absence of suitable conditions for diatom growth, the main biological response came from a
301 modest increase in picophytoplankton biomass but without an increase in particulate organic

302 carbon (POC). Growth was thought to have been kept in check by the resident
303 microzooplankton grazers with the increase in POC being recycled through the microbial food
304 web. In the patch, growth generally exceeded biomass except during the middle of the
305 experiment (D5-7) with high grazing on eukaryotic picoplankton during the first 7 days
306 (Peloquin et al., 2010a). Law *et al.* (2010) found that the mean net algal growth:dilution rate
307 of 1.13 (0.4-2.2) is the lowest reported for a FeAx, underpinning the importance of dilution in
308 SAGE. However the dilution rate decreased for Day 10-14 and growth exceeded grazing for
309 the total picophytoplankton and picoprokaryotes from D11.6 until the end of the experiment
310 (D15). We conclude, therefore that a combination of biological (grazing) and physical
311 (dilution rate) factors were important in limiting biomass accumulation in the treated patch.

312

313 Consistent with the limited biological response, the change in biologically influenced climate
314 relevant gases (CO₂ and DMS) was small (Figure 6f). Any enhanced biological draw-down
315 of pCO₂ was masked by a general increase in pCO₂ in the patch and mixing with higher pCO₂
316 waters to the west (Currie et al., 2010) during the period of intrusion. In the final phase of the
317 patch occupation, the median or mean in-patch CO₂ fugacity never dropped more than 1 μatm
318 below the OUT patch value. The cycling of sulfur components is discussed by Archer *et al.*
319 (2010). Any enhancement in production of dimethylsulfoniopropionate (DMSP) appears to
320 have been kept in check through grazing activity and, in contrast to most other iron
321 fertilisation experiments, the dissolved dimethylsulfide (DMS) concentration actually
322 declined over the course of the experiment.

323

324 **Comparisons and concluding remarks**

325 The ocean physics component of SAGE investigated processes important for gas exchange
326 estimation at strong windspeeds where the commonly used windspeed-based
327 parameterisations diverge. The SAGE dual-tracer gas exchange experiment was successful in
328 obtaining measurements under the highest average windspeed conditions (up to 16 m s⁻¹)
329 sampled to date, as described in Ho *et al.* (2006) and in Smith *et al.*, (2010). From re-
330 examination of previous dual-tracer experiments along with the SAGE measurements, Ho *et al.*
331 (2006) found that a quadratic relationship $k = 0.266 u_{10}^2 (600/Sc)^{0.5}$ accurately described
332 gas transfer for SAGE and previous dual-tracer datasets for the entire windspeed range. Here
333 k is gas transfer velocity, u_{10} is the windspeed 10 metres above the surface estimated from
334 QuikSCAT satellite derived winds, and Sc the Schmidt number used for normalisation with
335 600 being the Schmidt number for CO₂ in freshwater at 20°C. In contrast, the Liss and
336 Merlivat (1986) relationship significantly underestimated and the Wanninkhof and McGillis
337 (1999) cubic relationship significantly overestimated exchange. Ho *et al.* (2006) suggest that

338 their function is applicable to the entire global ocean including both the coastal and open
339 ocean environments. Smith *et al.* (2010) examine the influence of uncertainty and error in
340 windspeed (u) measurement on the gas-transfer velocity (k) windspeed relationship, and
341 considered the sea-state properties that can be used for refining estimates for strong winds e.g.
342 when bubble mediated transfer can be significant. Minnett *et al.* (2010) made skin
343 temperature measurements at higher windspeeds during SAGE than previously reported and
344 suggest that skin temperature is a more relevant temperature for input to gas exchange
345 estimation than bulk ocean temperature. The impact of skin versus bulk temperature on gas
346 exchange estimation is further examined by Currie *et al.* (2010).

347

348 Following the synthesis of de Baar *et al.* (2005) we compare the outcome of SAGE with other
349 iron addition experiments (FeAX's). Figure 10 shows the trend of increasing $\Delta f\text{CO}_2$, i.e. the
350 difference between IN and OUT patch CO_2 fugacity, with increasing surface chlorophyll a
351 biomass. The SEEDS experiment (Tsuda *et al.*, 2003) produced a very large draw-down
352 through a centric diatom bloom that developed in a very shallow surface mixed layer; by
353 comparison SAGE had a negligible impact in a deep mixed layer. Figure 11 shows SAGE
354 and SEEDS at the extremes of the range of response in chlorophyll concentrations in relation
355 to the range of mixed layer depths encountered in mesoscale iron addition experiments.

356

357 It is instructive to compare the biological responses in SAGE with the SEEDS II experiment
358 which was published after the de Baar *et al.* (2005) synthesis. SEEDS II was conducted in a
359 more diffusive ocean with a deeper mixed-layer depth and windier atmosphere resulting in a
360 much smaller response compared to the first SEEDS (Tsumune *et al.*, 2009). In both SAGE
361 and SEEDS II, picoplankton are an important component of the total assemblage. In SEEDS
362 II the picoplankton biomass (sized as 0.2 or 0.7 to 2.0 μm) of 0.17 mg m^{-3} initially accounts
363 for ~a quarter of the surface Chl- a . The picoplankton biomass increased substantially (1.1
364 mg m^{-3}); at Day 10 and accounts for an increased proportion (40%) of the surface Chl- a
365 (Kudo *et al.*, 2009). The trend continues in the decline phase with picoplankton accounting
366 for 65% of the surface Chl- a after 25 days. In SAGE, the initial picoplankton Chl- a amount
367 and proportion is substantially larger than in SEEDS II (0.47 mg m^{-3} and ~70%) (Peloquin *et al.*
368 *et al.*, 2010b) and whilst the Chl- a reaches 0.9 mg m^{-3} by Day 15, the dominant proportion
369 around 65-70% remains almost unchanged. Under the ecumenical iron hypothesis (Cullen,
370 1995; Morel *et al.*, 1991) it is proposed that small cells with high surface to volume ratio are
371 less sensitive to iron limitation and likely to be more sensitive to grazing controls. The results
372 from SAGE do not contradict this hypothesis where picoplankton biomass increased when
373 grazing pressure is reduced (Peloquin *et al.*, 2010b). In both experiments, diatoms did not
374 bloom. Initially in SEEDS II diatoms were the second most abundant of larger plankton

375 (Suzuki et al., 2009), and as the assemblage evolved, there tended to be a dominance of
376 grazing resistant species (Tsuda et al., 2009). However, Tsuda *et al.* (2007) reported an
377 exponential increase in copepod mesozooplankton, with copepod grazing representing a
378 major factor that prevented the formation of a diatom bloom. By contrast (Peloquin et al.,
379 2010b) found that diatoms comprised less than 1% of the initial biomass of SAGE and there
380 was no evidence of increase through the experiment. Whilst at first sight, this finding appears
381 to contradict the ecumenical iron hypothesis with the expectation of floristic shifts following
382 iron fertilisation, allowing diatoms that are less grazing dependent to bloom, it does agree
383 with the broader principle behind the hypothesis which suggests that no single factor will
384 regulate bloom development.

385

386 The biological response of SAGE was unexpected, representing a minimum end member
387 amongst the FeAX's conducted to date (Boyd et al., 2007), and has provided an excellent
388 framework for the study of multiple factors limiting primary productivity (Peloquin et al.,
389 2010a). The findings support and extend the analysis of de Baar *et al.* (2005) in the
390 relationship between response to iron addition and depth of the wind-mixed layer. Peloquin
391 et al (2010a; 2010b) suggest the system was only on the verge of light limitation and
392 important limiting factors included an active zooplankton grazing community and the diluting
393 effects of strong horizontal and vertical mixing. Furthermore, a diatom bloom in a HNLSiLC
394 region was unlikely because of the small (1%) initial diatom biomass and the low Si:N
395 nutrient status, especially later in the growing season following the seasonal drawdown of
396 macro-nutrients.

397

398 SAGE has demonstrated that iron fertilisation will not produce a response in all HNLC
399 regions at all times. In addition to the small response, conditions favoured the dominance of
400 picophytoplankton $< 2 \mu\text{m}$ (Peloquin et al., 2010b) which might suggest that any iron-
401 mediated gain of carbon is most likely to stay in the mixed-layer and be remineralised rather
402 than sink and be sequestered in the deep ocean. This leads us to suggest that seasonal effects,
403 HNLC sub-type (*e.g.* HNLSiLC) as well as ecosystem factors all need to be considered in
404 large-scale global models of iron fertilisation and in projected estimates of the ocean carbon
405 sink resulting from any large-scale ocean fertilisation (Browman and Boyd, 2009).

406

407 In planning this work, the SOLAS programme provided the case for integration of physical
408 and biological process studies to develop understanding of biologically driven air-sea gas
409 exchange. In conducting the broad-ranging SAGE experiment in the challenging environment
410 of the southern oceans, logistical capabilities were close to the limit of what is achievable
411 with a single vessel. For future multidisciplinary studies of this type, there are clear benefits

412 in the development of experimental design with multiple platforms, as has since been
413 demonstrated with some of the longer duration FeAX's.

414

415 **Acknowledgements**

416 This challenging experiment was made possible through the high quality of logistic support
417 provided by the entire crew of R.V. Tangaroa and personnel at NIWA Vessels Ltd. We thank
418 Greg Foothead for his lead with logistics co-ordination. SAGE was jointly funded through
419 the New Zealand Foundation for Research, Science and Technology (FRST) programs
420 (C01X0204) "Drivers and Mitigation of Global Change" and (C01X0223) "Ocean
421 Ecosystems: Their Contribution to NZ Marine Productivity," Funding was also provided for
422 specific collaborations by the US National Science Foundation from grants OCE-0326814
423 (Ward), OCE-0327779 (Ho), and OCE 0327188 OCE-0326814 (Minnett) and the UK Natural
424 Environment Research Council NER/B/S/2003/00282 (Archer). The New Zealand
425 International Science and Technology (ISAT) linkages fund provided additional funding
426 (Archer and Ziolkowski), and the many collaborator institutions also provided valuable
427 support.

428

429 **Figure legends**

430 Figure 1: Bathymetry map to the south-east of New Zealand in the vicinity of the SAGE
431 experiment. Depth (meters) is indicated by the colour bar.

432

433 Figure 2: SeaWiFS chlorophyll *a* composite Mar – Apr 2004. SAGE site is shown as a red
434 dot.

435

436 Figure 3: Timeline of SeaWiFS chlorophyll *a* for SAGE site, extracted from 8 day composite
437 standard mapped images. Statistics are for a tile of up to 48 pixels (approx 50 x 50 km)
438 centred on 46.5°S 172.5°E. The vertical arrow marks the time of the SAGE experiment.

439

440 Figure 4: Sea surface height plot for 24 March 2004 from AVISO delayed-time, reference,
441 merged, Mapped Sea Level Anomalies (MSLA_DT_REF) from sea level anomaly data set at
442 0.25° × 0.25° derived from satellite altimeters on TOPEX/Poseidon and ERS satellites
443 www.aviso.oceanobs.com and NRL Coastal Ocean Model Sea Surface Height Mean. Release
444 site is centred on the white dot. Anomaly (m) is indicated by the colour bar.

445

446 Figure 5: Geostrophic current velocity calculated from SSH for 3 April 2004, data source as
447 in Figure 4 (Hadfield, 2010). The yellow line shows the entire voyage track which
448 progressed in an anti-clockwise direction. Current barbs show direction, filled contours show
449 speed (m s⁻¹): 0–0.05 white, 0.05–0.10 light grey, 0.10–0.20 darker grey, 0.20–0.30 blue,
450 0.30–0.40 navy.

451

452 Figure 6: Evolution of the SAGE fertilised patch. Variables in the left column were measured
453 from daily CTD casts, where Day 0 is the night 25/26 March (19:00 25-Mar-2004 for
454 continuous data). The vertical arrows show the mid-times of the four iron infusions. Variables
455 in the right column are from continuous underway seawater sampling where samples are
456 assigned as IN patch from SF₆ tracer levels above 10 fM and are otherwise regarded as OUT
457 patch (a) Surface (top 10 m) nitrate and silicate concentrations IN and OUT of the patch. (b)
458 Median surface (2 m) dissolved iron measured from towed torpedo trace iron sampler. The
459 vertical bars extend between minimum and maximum values. (c) Total euphotic zone
460 chlorophyll-a by trapezoidal integration to the 0.5 % light level as mean and standard error as
461 calculated by Peloquin et al. (2010b). (d) Photosynthetic competence F_v/F_m measured at
462 night. Vertical bars show the mean and standard deviation for each night-time. (e) Total
463 euphotic zone primary productivity by trapezoidal integration to the 0.5 % light level as mean
464 and standard error as calculated by Peloquin et al. (2010b). (f) Median fugacity of CO₂. The
465 vertical bars extend between minimum and maximum values.

466

467 Figure 7: Median, maximum and minimum daily u_{10} windspeed calculated from vessel
468 anemometer and corrected for flow distortion according to Popinet *et al.* (2004). The dashed
469 bar to the left shows a horizontal mark at the median and extends from the 5th to the 99th
470 percentile of ship windspeed observations presented by Hadfield (2010).

471

472 Figure 8: Measured and theoretical maximum clear sky daily incident photosynthetically
473 active radiation calculated with an atmospheric transmission coefficient of 0.86 and top of the
474 atmosphere PAR of 2500 $\mu\text{mol m}^{-2} \text{s}^{-1}$. Inverted triangles are 8-day composite surface PAR
475 from SeaWIFS for 1°x1° box including the SAGE site presented by Hadfield (2010).

476

477 Figure 9: Comparison of light availability in iron addition experiments. The black bars show
478 the range of theoretical maximum clear sky daily incident PAR calculated with an
479 atmospheric transmission coefficient of 0.86 and top of the atmosphere PAR of flux of
480 2500 $\mu\text{mol m}^{-2} \text{s}^{-1}$. The box plots show the range, quartiles and median of surface PAR
481 (allowing for cloudiness) based on 8-day composite SeaWIFS PAR estimate (Frouin et al.,
482 2003) for a 7 x 7 tile of pixels at 9-km resolution over the duration of each experiment.

483

484 Figure 10: A comparison of the maximum IN:OUT patch difference in $f\text{CO}_2$ versus the
485 maximum surface chlorophyll for a number of FeAX's. Data sources are from Boyd et al.
486 (2007) including supplemental tables. In addition SEEDSII data are from (Tsumune et al.,
487 2009) and KEOPS data from a study of natural iron fertilisation on the Kerguelen Plateau
488 (Blain et al., 2007).

489

490 Figure 11: The enhancement in surface chlorophyll *a* ranked in approximate order of
491 reducing mixed-layer depth for 10 FeAX's (note IronEx-1 did not evolve due to patch
492 subduction after 4 days). Adapted from de Baar et al (2005), with inclusion of data from
493 SEEDS II and SAGE (Boyd et al., 2007 Suppl. tables).

494

495 **Tables**

496

Variable ± stdev	Initial condition
SST (°C)	11.5 ± 0.05
Salinity	34.316 ± 0.003
Background dissolved Fe (nM)	0.09 ± 0.005
Surface NO ₃ range (µM)	7.6 – 10.3
Surface SiO ₄ range (µM)	0.83 - 0.97
Dissolved reactive phosphorus (µM)	0.62 – 0.85
Fv/Fm	0.27 ± 0.02
Primary Productivity (mmolCm ⁻³ d ⁻¹)	0.53 ± 0.02
Biology	Picophytoplankton dominated
3 hour prior wind (ms ⁻¹)	10.7 ± 1.1
“Mixed-layer depth” (m)	~60
Surface chlorophyll <i>a</i> (mg m ⁻³)	0.64 ± 0.05
Integrated chlorophyll <i>a</i> (mg m ⁻²)	44.4 ± 1.5
pCO ₂ (µatm)	327.3 ± 2.0

497

498 Table 1: Summary of initial conditions at the SAGE first release site 46° 44’S 172° 32’E with

499 seawater sampled from ships scientific supply (5 m depth)

500

Infusion	Date (NZST)	Tracer added	Fe added	Flow rate		Ship speed kts	Post infusion Fe nM
			kg (Fe)	L h ⁻¹			
1	25/03/04 1500 – 2330	SF ₆ & ³ He	265	Fe	925 Lh ⁻¹	4.25	3.03
				SF ₆ & ³ He	475 Lh ⁻¹		
2	31/03/04 0000 – 0600	SF ₆ & ³ He	265	Fe	1370 Lh ⁻¹	5.5	1.59
				SF ₆ & ³ He	690 Lh ⁻¹		
3	03/04/04 1230 – 1830		265	Fe	1200 Lh ⁻¹	7-8	0.55
4	06/04/04 2220 - 0330	SF ₆	265	Fe	1200 Lh ⁻¹	5-6	1.01
				SF ₆	500 Lh ⁻¹		

501

502 Table 2: SAGE infusion details

503

504 **References**

505

506 Archer, S.D., Safi, K., Hall, J.A., Cummings, D.G., Harvey, M., 2010. Grazing suppression of
507 dimethylsulphoniopropionate (DMSP) accumulation in iron fertilised sub-Antarctic waters.
508 Deep Sea Research Part II: Topical Studies in Oceanography.

509 Bathmann, U., 2005. Ecological and biogeochemical response of Antarctic ecosystems to iron
510 fertilization and implications on global carbon cycle. Ocean and Polar Research 27, 231-235.

511 Blain, S., Quéguiner, B., Armand, L., Belviso, S., Bombled, B., Bopp, L., Bowie, A., Brunet,
512 C., Brussaard, C., Carlotti, F., Christaki, U., Corbière, A., Durand, I., Ebersbach, F., Fuda, J.-
513 L., Garcia, N., Gerringa, L., Griffiths, B., Guigue, C., Guillerm, C., Jacquet, S., Jeandel, C.,

- 514 Laan, P., Lefèvre, D., Lo Monaco, C., Malits, A., Mosseri, J., Obernosterer, I., Park, Y.-H.,
515 Picheral, M., Pondaven, P., Remenyi, T., Sandroni, V., Sarthou, G., Savoye, N., Scouarnec,
516 L., Souhaut, M., Thuiller, D., Timmermans, K., Trull, T., Uitz, J., van Beek, P., Veldhuis, M.,
517 Vincent, D., Viollier, E., Vong, L., Wagener, T., 2007. Effect of natural iron fertilization on
518 carbon sequestration in the Southern Ocean. *Nature* 446, 1070-1074.
- 519 Blain, S., Treguer, P., Belviso, S., Bucciarelli, E., Denis, M., Desabre, S., Fiala, M., Martin
520 Jezequel, V., Le Fevre, J., Mayzaud, P., 2001. A biogeochemical study of the island mass
521 effect in the context of the iron hypothesis: Kerguelen Islands, Southern Ocean. *Deep Sea*
522 *Research Part I: Oceanographic Research Papers* 48, 163-187.
- 523 Boyd, P., LaRoche, J., Gall, M., Frew, R., McKay, R.M.L., 1999. Role of iron, light, and
524 silicate in controlling algal biomass in subantarctic waters SE of New Zealand. *J. Geophys.*
525 *Res.* 104, 13395-13408.
- 526 Boyd, P.W., Abraham, E.R., 2001. Iron-mediated changes in phytoplankton photosynthetic
527 competence during SOIREE. *Deep-Sea Research Part II: Topical Studies in Oceanography*
528 48, 2529-2550.
- 529 Boyd, P.W., Jickells, T., Law, C.S., Blain, S., Boyle, E.A., Buesseler, K.O., Coale, K.H.,
530 Cullen, J.J., de Baar, H.J.W., Follows, M., Harvey, M., Lancelot, C., Levasseur, M., Owens,
531 N.P.J., Pollard, R., Rivkin, R.B., Sarmiento, J., Schoemann, V., Smetacek, V., Takeda, S.,
532 Tsuda, A., Turner, S., Watson, A.J., 2007. Mesoscale Iron Enrichment Experiments 1993-
533 2005: Synthesis and Future Directions. *Science* 315, 612-617.
- 534 Boyd, P.W., Law, C.S., Abraham, E.R., Hadfield, M., Hill, P., Oliver, M., Pinkerton, M.,
535 Smith, M., Hutchins, D.A., Handy, S., Hare, C., LeBlanc, K., Croot, P.L., Ellwood, M., Hall,
536 J., Pickmere, S., Safi, K., Frew, R.D., Hunter, K.A., Sander, S., Strzepek, R., Higgins, J.,
537 Mioni, C., Wilhelm, S.W., Maldonado, M.T., McKay, R.M., Sanudo-Wilhelmy, S.A., Tovar-
538 Sanchez, A., 2005. FeCycle: Attempting an iron biogeochemical budget from a mesoscale
539 SF6 tracer experiment in unperturbed low iron waters. *Global Biogeochem. Cycles* 19, doi:
540 10.1029/2005GB002494.
- 541 Boyd, P.W., Law, C.S., Wong, C.S., Nojiri, Y., Tsuda, A., Levasseur, M., Takeda, S., Rivkin,
542 R., Harrison, P.J., Strzepek, R., Gower, J., McKay, R.M., Abraham, E., Arychuk, M.,
543 Barwell-Clarke, J., Crawford, W., Crawford, D., Hale, M., Harada, K., Johnson, K.,
544 Kiyosawa, H., Kudo, I., Marchetti, A., Miller, W., Heedoba, J., Nishioka, J., Ogawa, H., Page,
545 J., Robert, M., Saito, H., Sastri, A., Sherry, H., Soutar, T., Sutherland, N., Taira, Y., Whitney,
546 F., Wong, S.K.E., Yoshimura, T., 2004. The decline and fate of an iron-induced subarctic
547 phytoplankton bloom. *Nature* 428, 549-553.
- 548 Boyd, P.W., Watson, A.J., Law, C.S., Abraham, E.R., Trull, T., Murdoch, R., Bakker, D.C.E.,
549 Bowie, A.R., Buesseler, K.O., Chang, H., Charette, M., Croot, P., Downing, K., Frew, R.,
550 Gall, M., Hadfield, M., Hall, J., Harvey, M., Jameson, G., LaRoche, J., Liddicoat, M., Ling,
551 R., Maldonado, M.T., McKay, R.M., Nodder, S., Pickmere, S., Pridmore, R., Rintoul, S., Safi,
552 K., Sutton, P., Strzepek, R., Tanneberger, K., Turner, S., Waite, A., Zeldis, J., 2000. A
553 mesoscale phytoplankton bloom in the polar Southern Ocean stimulated by iron fertilisation.
554 *Nature* 407, 695-702.
- 555 Browman, H., Boyd, P.W., 2009. Theme Section: Implications of large-scale iron
556 fertilization of the oceans. *Mar Ecol Prog Ser* 364, 213-309.
- 557 Brzezinski, M.A., Jones, J.L., Demarest, M.S., 2005. Control of silica production by iron and
558 silicic acid during the Southern Ocean Iron Experiment (SOFeX). *Limnol Oceanogr* 50, 810-
559 824.

- 560 Buesseler, K.O., Boyd, P.W., 2003. Will Ocean Fertilization Work? *Science* 300, 67-68.
- 561 Buesseler, K.O., Doney, S.C., Karl, D.M., Boyd, P.W., Caldeira, K., Chai, F., Coale, K.H., De
562 Baar, H.J.W., Falkowski, P.G., Johnson, K.S., Lampitt, R.S., Michaels, A.F., Naqvi, S.W.A.,
563 Smetacek, V., Takeda, S., Watson, A.J., 2008. Environment: Ocean iron fertilization -
564 Moving forward in a sea of uncertainty. *Science* 319, 162.
- 565 Canadell, J.G., Le Quéré, C., Raupach, M.R., Field, C.B., Buitenhuis, E.T., Ciais, P., Conway,
566 T.J., Gillett, N.P., Houghton, R.A., Marland, G., 2007. Contributions to accelerating
567 atmospheric CO₂ growth from economic activity, carbon intensity, and efficiency of natural
568 sinks. *Proc Natl Acad Sci U S A* 104, 18866-18870.
- 569 Carr, M.-E., Tang, W., Liu, W.T., 2002. CO₂ exchange coefficients from remotely sensed
570 wind speed measurements: SSM/I versus QuikSCAT in 2000 doi:10.1029/23002GL015068.
571 *Geophys. Res. Lett.* 29, 30-31.
- 572 Coale, K.H., Johnson, K.S., Chavez, F.P., Buesseler, K.O., Barber, R.T., Brzezinski, M.A.,
573 Cochlan, W.P., Millero, F.J., Falkowski, P.G., Bauer, J.E., Wanninkhof, R.H., Kudela, R.M.,
574 Altabet, M.A., Hales, B.E., Takahashi, T., Landry, M.R., Bidigare, R.R., Wang, X., Chase, Z.,
575 Strutton, P.G., Friederich, G.E., Gorbunov, M.Y., Lance, V.P., Hilting, A.K., Hiscock, M.R.,
576 Demarest, M., Hiscock, W.T., Sullivan, K.F., Tanner, S.J., Gordon, R.M., Hunter, C.N.,
577 Elrod, V.A., Fitzwater, S.E., Jones, J.L., Tozzi, S., Koblizek, M., Roberts, A.E., Herndon, J.,
578 Brewster, J., Ladizinsky, N., Smith, G., Cooper, D., Timothy, D., Brown, S.L., Selph, K.E.,
579 Sheridan, C.C., Twining, B.S., Johnson, Z.I., 2004. Ocean Science: Southern Ocean Iron
580 Enrichment Experiment: Carbon Cycling in High- and Low-Si Waters. *Science* 304, 408-414.
- 581 Coale, K.H., Johnson, K.S., Fitzwater, S.E., Gordon, R.M., Tanner, S., Chavez, F.P., Ferioli,
582 L., Sakamoto, C., Rogers, P., Millero, F., Steinberg, P., Nightingale, P., Cooper, D.,
583 Cochlamn, W.P., Landry, M.R., Constantinou, J., RollwagenG, Trasvina, A., Kudela, R.,
584 1996. A massive phytoplankton bloom induced by an ecosystem-scale iron fertilisation
585 experiment in the equatorial Pacific Ocean. *Nature* 383, 495-508.
- 586 Cullen, J.J., 1995. Status of the iron hypothesis after the Open-Ocean Enrichment Experiment.
587 *Limnol Oceanogr* 40, 1336-1343.
- 588 Currie, K.I., Macaskill, B., Reid, M.R., Law, C.S., 2010. Processes governing the carbonate
589 chemistry during the SAGE experiment. *Deep Sea Research Part II: Topical Studies in*
590 *Oceanography*.
- 591 D'Asaro, E., McNeil, C., 2008. Air-sea gas exchange at extreme wind speeds measured by
592 autonomous oceanographic floats. *Journal of Marine Systems* 74, 722-736.
- 593 de Baar, H.J.W., Boyd, P.W., Coale, K.H., Landry, M.R., Tsuda, A., Assmy, P., Bakker,
594 D.C.E., Bozec, Y.T., Barber, R.T., Brzezinski, M.A., Buesseler, K.O., Boyé, M., Croot, P.L.,
595 Gervais, F., Gorbunov, M.Y., Harrison, P.J.T., Hiscock, W.T., Laan, P., Lancelot, C., Law,
596 C.S., Levasseur, M., Marchetti, A., Millero, F.J., Nishioka, J., Nojiri, Y., van Oijen, T.,
597 Riebesell, U., Rijkenberg, M.J.A., Saito, H., Takeda, S., Timmermans, K.R., Veldhuis,
598 M.J.W., Waite, A.M., Wong C.-S., 2005. Synthesis of iron fertilization experiments: From the
599 Iron Age in the Age of Enlightenment. *J. Geophys. Res.* 110, doi:10.1029/2004JC002601.
- 600 Dugdale, R.C., Wilkerson, F.P., 1998. Silicate regulation of new production in the equatorial
601 Pacific upwelling. *Nature* 391, 270-273.

602 Fairall, C.W., Hare, J.E., Edson, J.B., McGillis, W., 2000. Parameterization and
603 micrometeorological measurement of air-sea gas transfer. *Boundary-Layer Meteorology* 96,
604 63-105.

605 Feely, R.A., Cosca, C.E., Wanninkhof, R., McGillis, W., Carr, M.-E., 2004. Effects of wind
606 speed and gas exchange parameterizations on the air-sea CO₂ fluxes in the equatorial Pacific
607 Ocean. *Journal of Geophysical Research C: Oceans* 109, 10.1029/2003JC001896.

608 Frouin, R., Franz, B.A., Werdell, P.J., 2003. The SeaWiFS PAR product. NASA Technical
609 Memorandum - SeaWiFS Postlaunch Technical Report Series, 46-50.

610 Hadfield, M., 2010. Predicted and observed conditions during the SAGE Iron Addition
611 experiment in Sub-Antarctic Waters. *Deep Sea Research Part II: Topical Studies in*
612 *Oceanography*.

613 Ho, D.T., Law, C.S., Smith, M.J., Schlosser, P., Harvey, M., Hill, P., 2006. Measurements of
614 air-sea gas exchange at high wind speeds in the Southern Ocean: Implications for global
615 parameterizations. doi:10.1029/2006GL026817. *Geophys. Res. Lett.* 33, L16611.

616 Kudo, I., Noiri, Y., Cochlan, W.P., Suzuki, K., Aramaki, T., Ono, T., Nojiri, Y., 2009.
617 Primary productivity, bacterial productivity and nitrogen uptake in response to iron
618 enrichment during the SEEDS II. *Deep-Sea Research Part II-Topical Studies in Oceanography*
619 56, 2755-2766.

620 Kuparinen, J., Hall, J., Ellwood, M., Safi, K., Peloquin, J., Katz, D., 2010. Bacterioplankton
621 responses to iron enrichment during SOLAS-SAGE experiment. *Deep Sea Research Part II:*
622 *Topical Studies in Oceanography*.

623 Law, C.S., Smith, M., Stevens, C., Abraham, E.R., Ellwood, M., Hill, P., Nodder, S.,
624 Peloquin, J., Pickmere, S., Safi, K., Walkington, M., 2010. Did dilution limit the
625 phytoplankton response to iron addition in HNLCLS Sub-Antarctic waters during SAGE?
626 *Deep Sea Research Part II: Topical Studies in Oceanography*.

627 Law, R.M., Matear, R.J., Francey, R.J., 2008. Comment on "Saturation of the Southern Ocean
628 CO₂ Sink Due to Recent Climate Change". *Science* 319, 570a.

629 Le Quéré, C., Rödenbeck, C., Buitenhuis, E.T., Conway, T.J., Langenfelds, R., Gomez, A.,
630 Labuschagne, C., Ramonet, M., Nakazawa, T., Metzl, N., Gillett, N., Heimann, M., 2007.
631 Saturation of the Southern Ocean CO₂ Sink Due to Recent Climate Change. *Science* 316,
632 1735-1738.

633 Lenton, T.M., Vaughan, N.E., 2009. The radiative forcing potential of different climate
634 geoengineering options. *Atmospheric Chemistry and Physics Discussions* 9, 2559-2608.

635 Liss, P.S., 1983. Gas Transfer: Experiments and geochemical implications., in: Liss, P.S.,
636 Slinn, W.G.N. (Eds.), *Air-Sea Exchange of Gases and Particles*. Reidel, pp. 241-298.

637 Liss, P.S., Merlivat, L., 1986. Air-sea gas exchange rates: introduction and synthesis, in:
638 Buat-Ménard, P. (Ed.), *The role of air-sea exchange in geochemical cycling*. D.Reidel,
639 Dordrecht, pp. 113-127.

640 Martin, J.H., Gordon, R.M., Fitzwater, S.E., 1990. Iron in Antarctic waters. *Nature* 345, 156-
641 158.

- 642 Minnett, P.J., Smith, M., Ward, B., 2010. Measurements of the oceanic thermal skin effect.
643 Deep Sea Research Part II: Topical Studies in Oceanography.
- 644 Mokhov, I.I., Schlesinger, M.E., 1994. Analysis of global cloudiness 2. Comparison of
645 ground-based and satellite-based cloud climatologies. *J. Geophys. Res.* 99, 17045-17065.
- 646 Morel, F.M.M., Rueter, J.G., Price, N.M., 1991. Iron nutrition of phytoplankton and its
647 possible importance in the ecology of ocean regions with high nutrient and low biomass.
648 *Oceanography* 4, 56-61.
- 649 Nightingale, P.D., Malin, G., Law, C.S., Watson, A.J., Liss, P.S., Liddicoat, M.I., Boutin, J.,
650 Upstill-Goddard, R.C., 2000. In situ evaluation of air-sea gas exchange parameterisations
651 using novel conservative tracers. *Global Biogeochem. Cycles* 27, 2117-2120.
- 652 Olsen, A., Wanninkhof, R., Trinanes, J.A., Johannessen, T., 2005. The effect of wind speed
653 products and wind speed-gas exchange relationships on interannual variability of the air-sea
654 CO₂ gas transfer velocity. *Tellus Ser B Chem Phys Meteorol* 57, 95-106.
- 655 Peloquin, J., Hall, J., Safi, K., Ellwood, M., Law, C.S., Thompson, K., Kuparinen, J., Harvey,
656 M., Pickmere, S., 2010a. Control of the phytoplankton response during the SAGE experiment:
657 a synthesis. *Deep Sea Research Part II: Topical Studies in Oceanography*.
- 658 Peloquin, J., Hall, J., Safi, K., Smith Jr., W.O., Wright, S., van den Enden, R., 2010b. The
659 response of phytoplankton to iron enrichment in Sub-Antarctic HNLCLSi waters: results from
660 the SAGE experiment. *Deep Sea Research Part II: Topical Studies in Oceanography*.
- 661 Pollard, R.T., Salter, I., Sanders, R.J., Lucas, M.I., Moore, C.M., Mills, R.A., Statham, P.J.,
662 Allen, J.T., Baker, A.R., Bakker, D.C.E., Charette, M.A., Fielding, S., Fones, G.R., French,
663 M., Hickman, A.E., Holland, R.J., Hughes, J.A., Jickells, T.D., Lampitt, R.S., Morris, P.J.,
664 Nédélec, F.H., Nielsdóttir, M., Planquette, H., Popova, E.E., Poulton, A.J., Read, J.F.,
665 Seeyave, S., Smith, T., Stinchcombe, M., Taylor, S., Thomalla, S., Venables, H.J.,
666 Williamson, R., Zubkov, M.V., 2009. Southern Ocean deep-water carbon export enhanced by
667 natural iron fertilization. *Nature* 457, 577-580.
- 668 Popinet, S., Smith, M., Stevens, C., 2004. Experimental and Numerical Study of the
669 Turbulence Characteristics of Airflow around a Research Vessel. *Journal of Atmospheric and
670 Oceanic Technology* 21, 1575-1589.
- 671 Smith, M.J., Ho, D.T., Law, C.S., McGregor, J., Popinet, S., Schlosser, P., 2010.
672 Uncertainties in Gas Exchange Parameterization during the SAGE dual-tracer experiment.
673 *Deep Sea Research Part II: Topical Studies in Oceanography*.
- 674 Stevens, C., Ward, B., Law, C.S., Walkington, M., 2010. Surface layer mixing during SAGE
675 Ocean Fertilisation Experiment. *Deep Sea Research Part II: Topical Studies in Oceanography*.
- 676 Sura, P., 2003. Stochastic analysis of Southern and Pacific Ocean Sea Surface Winds. *Journal
677 of the atmospheric Sciences* 60, 654-666.
- 678 Suzuki, K., Saito, H., Isada, T., Hattori-Saito, A., Kiyosawa, H., Nishioka, J., McKay,
679 R.M.L., Kuwata, A., Tsuda, A., 2009. Community structure and photosynthetic physiology of
680 phytoplankton in the northwest subarctic Pacific during an in situ iron fertilization experiment
681 (SEEDS-II). *Deep-Sea Research Part II-Topical Studies in Oceanography* 56, 2733-2744.
- 682 Takahashi, T., Sutherland, S.C., Sweeney, C., Poisson, A., Metzl, N., Tilbrook, B., Bates, N.,
683 Wanninkhof, R., Feely, R.A., Sabine, C., Olafsson, J., Nojiri, Y., 2002. Global sea-air CO₂

684 flux based on climatological surface ocean pCO₂, and seasonal biological and temperature
685 effects. *Deep-Sea Res. II* 49, 1601-1622.

686 Takahashi, T., Sutherland, S.C., Wanninkhof, R., Sweeney, C., Feely, R.A., Chipman, D.W.,
687 Hales, B., Friederich, G., Chavez, F., Sabine, C., Watson, A., Bakker, D.C.E., Schuster, U.,
688 Metzl, N., Yoshikawa-Inoue, H., Ishii, M., Midorikawa, T., Nojiri, Y., Körtzinger, A.,
689 Steinhoff, T., Hoppema, M., Olafsson, J., Arnarson, T.S., Tilbrook, B., Johannessen, T.,
690 Olsen, A., Bellerby, R., Wong, C.S., Delille, B., Bates, N.R., de Baar, H.J.W., 2009.
691 Climatological mean and decadal change in surface ocean pCO₂, and net sea-air CO₂ flux
692 over the global oceans. *Deep-Sea Research Part II: Topical Studies in Oceanography*
693 doi:10.1016/j.dsr2.2008.12.009.

694 Trull, T., Rintoul, S.R., Hadfield, M., Abraham, E.R., 2001. Circulation and seasonal
695 evolution of polar waters south of Australia: implications for iron fertilization of the Southern
696 Ocean. *Deep Sea Research II* 48, 2439-2466.

697 Tsuda, A., Saito, H., Machida, R.J., Shimode, S., 2009. Meso- and microzooplankton
698 responses to an in situ iron fertilization experiment (SEEDS II) in the northwest subarctic
699 Pacific. *Deep-Sea Research Part II-Topical Studies in Oceanography* 56, 2767-2778.

700 Tsuda, A., Takeda, S., Saito, H., Nishioka, J., Kudo, I., Nojiri, Y., Suzuki, K., Uematsu, M.,
701 Wells, M.L., Tsumune, D., Yoshimura, T., Aono, T., Aramaki, T., Cochlan, W.P., Hayakawa,
702 M., Imai, K., Isada, T., Iwamoto, Y., Johnson, W.K., Kameyama, S., Kato, S., Kiyosawa, H.,
703 Kondo, Y., Levasseur, M., Machida, R.J., Nagao, I., Nakagawa, F., Nakanish, T., Nakatsuka,
704 S., Narita, A., Noiri, Y., Obata, H., Ogawa, H., Oguma, K., Ono, T., Sakuragi, T., Sasakawa,
705 M., Sato, M., Shimamoto, A., Takata, H., Trick, C.G., Watanabe, Y.W., Wong, C.S., Yoshie,
706 N., 2007. Evidence for the grazing hypothesis: Grazing reduces phytoplankton responses of
707 the HNLC ecosystem to iron enrichment in the western subarctic pacific (SEEDS II). *Journal*
708 *of Oceanography* 63, 983-994.

709 Tsuda, A., Takeda, S., Saito, H., Nishioka, J., Nojiri, Y., Kudo, I., Kiyosawa, H., Shiomoto,
710 A., Imai, K., Ono, T., Shimamoto, A., Tsumune, D., Yoshimura, T., Aono, T., Hinuma, A.,
711 Kinugasa, M., Suzuki, K., Sohrin, Y., Noiri, Y., Tani, H., Deguchi, Y., Tsurushima, N.,
712 Ogawa, H., Fukami, K., Kuma, K., Saino, T., 2003. A mesoscale iron enrichment in the
713 Western subarctic Pacific induces a large centric diatom bloom. *Science* 300, 958-961.

714 Tsumune, D., Nishioka, J., Shimamoto, A., Watanabe, Y.W., Aramaki, T., Nojiri, Y., Takeda,
715 S., Tsuda, A., Tsubono, T., 2009. Physical behaviors of the iron-fertilized patch in SEEDS II.
716 *Deep-Sea Research Part II-Topical Studies in Oceanography* 56, 2948-2957.

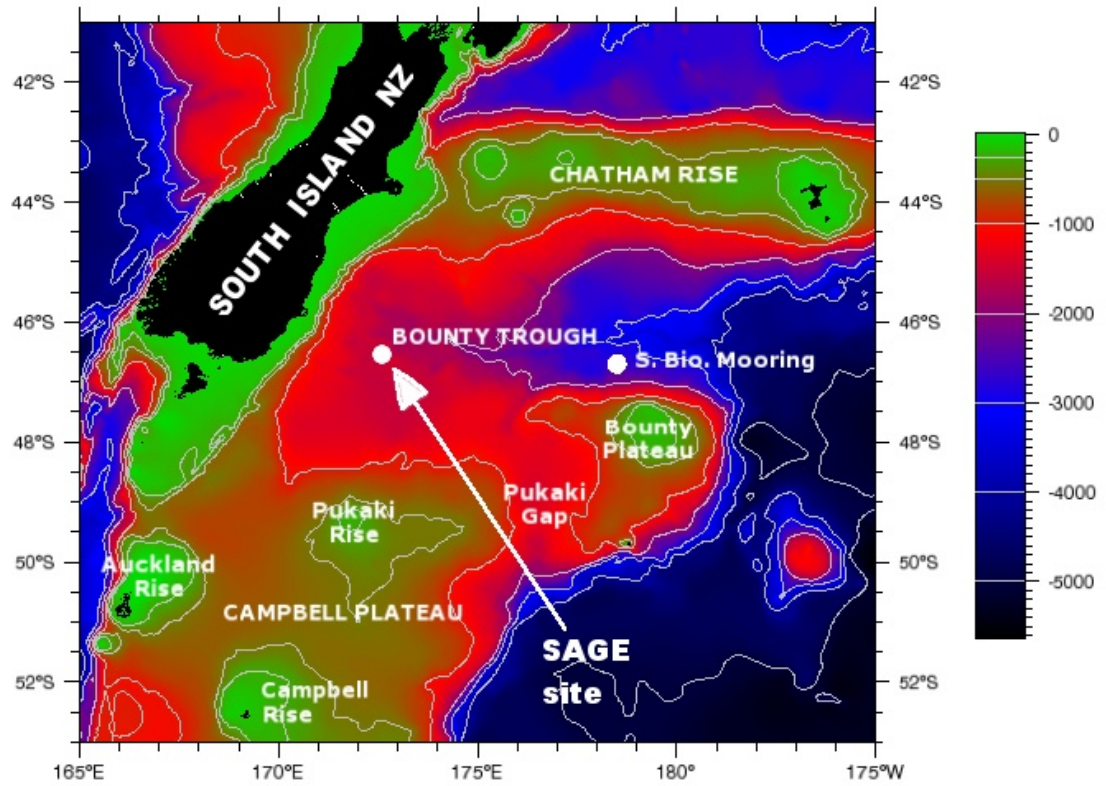
717 van Oijen, T., van Leeuwe, M.A., Granum, E., Weissing, F.J., Bellerby, R.G.J., Gieskes,
718 W.W.C., de Baar, H.J.W., 2004. Light rather than iron controls photosynthate production and
719 allocation in Southern Ocean phytoplankton populations during austral autumn. *J Plankton*
720 *Res* 26, 885-900.

721 Wanninkhof, R., 1992. Relationship between wind speed and gas exchange over the ocean. *J.*
722 *Geophys. Res.* 97, 7373-7382.

723 Wanninkhof, R., 1993. Gas transfer experiment on Georges Bank using two volatile
724 deliberate tracers. *J. Geophys. Res.* 98, 20237-20248.

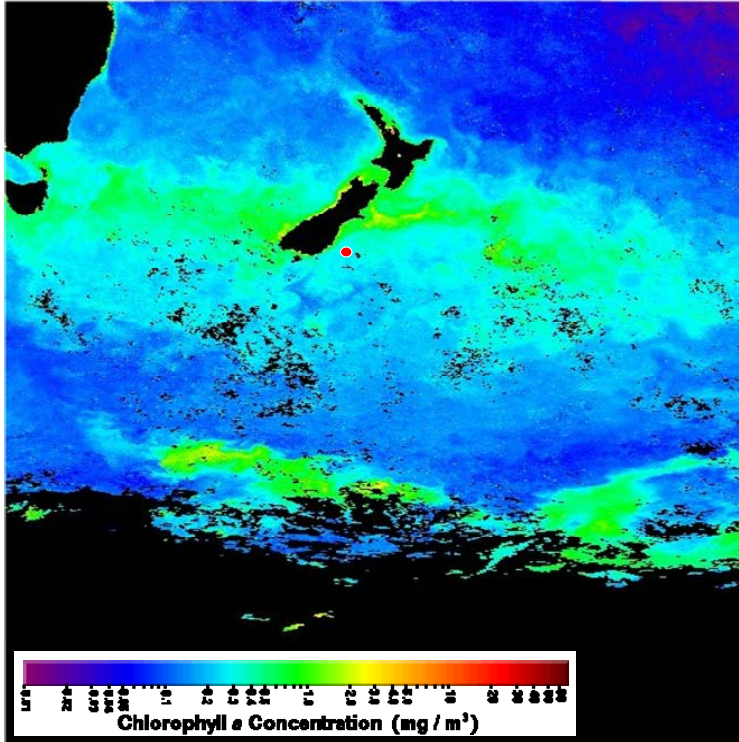
725 Wanninkhof, R., McGillis, W.R., 1999. A cubic relationship between air-sea CO₂ exchange
726 and wind speed. *Geophys. Res. Lett.* 26, 1889-1892.

- 727 Wanninkhof, R., Ortner, P.B., Zhang, J.-Z., Hitchcock, G., Wiseman, W.J., Vargo, G.,
728 Masserini, R., Fanning, K., Asher, W., Ho, D.T., Schlosser, P., Dickson, M.-L., 1997. Gas
729 exchange, dispersion, and biological productivity on the west Florida shelf: Results from a
730 Lagrangian tracer study. *Geophys. Res. Lett.* 24, 1767-1770.
- 731 Wanninkhof, R., Sullivan, K.F., Top, Z., 2004. Air-sea gas transfer in the Southern Ocean. *J.*
732 *Geophys. Res.* 109, doi:10.1029/2003JC001767.
- 733 Ward, B., Wanninkhof, R., McGillis, W.R., Jessup, A.T., DeGrandpre, M.D., Hare, J.E.,
734 Edson, J.B., 2004. Biases in the air-sea flux of CO₂ resulting from ocean surface temperature
735 gradients. *J. Geophys. Res.* 109, doi:10.1029/2003JC001800.
- 736 Woolf, D.K., 1997. Bubbles and their role in gas exchange, in: Liss, P.S., Duce, R.A. (Eds.),
737 *The Sea Surface and Global Change*. Cambridge University Press, Cambridge, pp. 173-205.
- 738 Zickfeld, K., Fyfe, J.C., Eby, M., Weaver, A.J., 2008. Comment on “Saturation of the
739 Southern Ocean CO₂ Sink Due to Recent Climate Change”. *Science* 319, 570b.
740
741
742



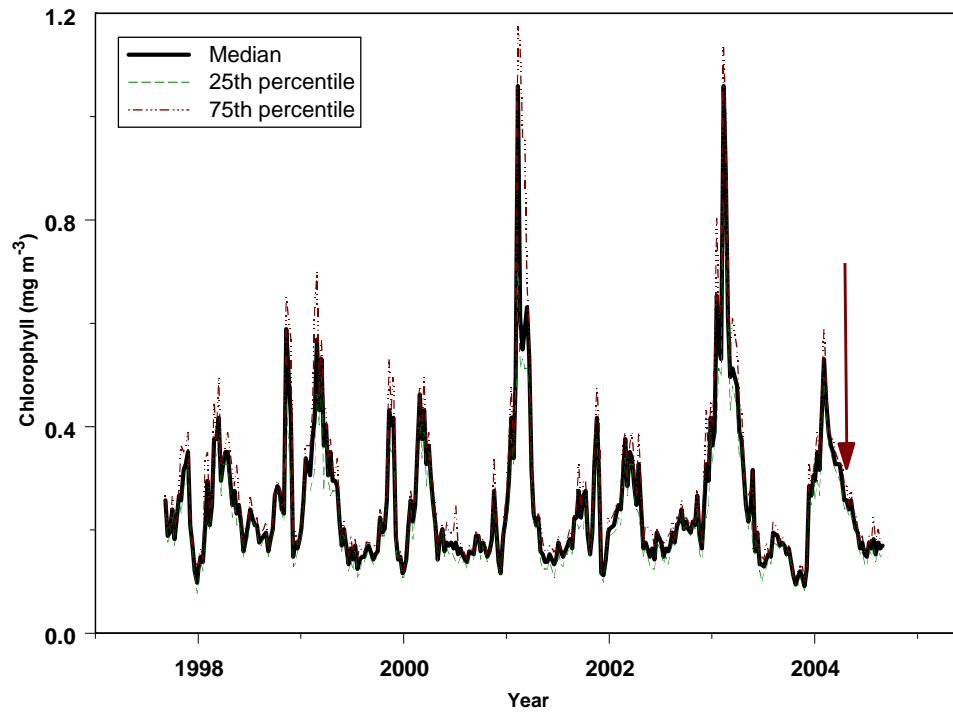
743
 744 Figure 1: Bathymetry map to the south-east of New Zealand in the vicinity of the SAGE
 745 experiment. Depth (meters) is indicated by the colour bar.
 746

747

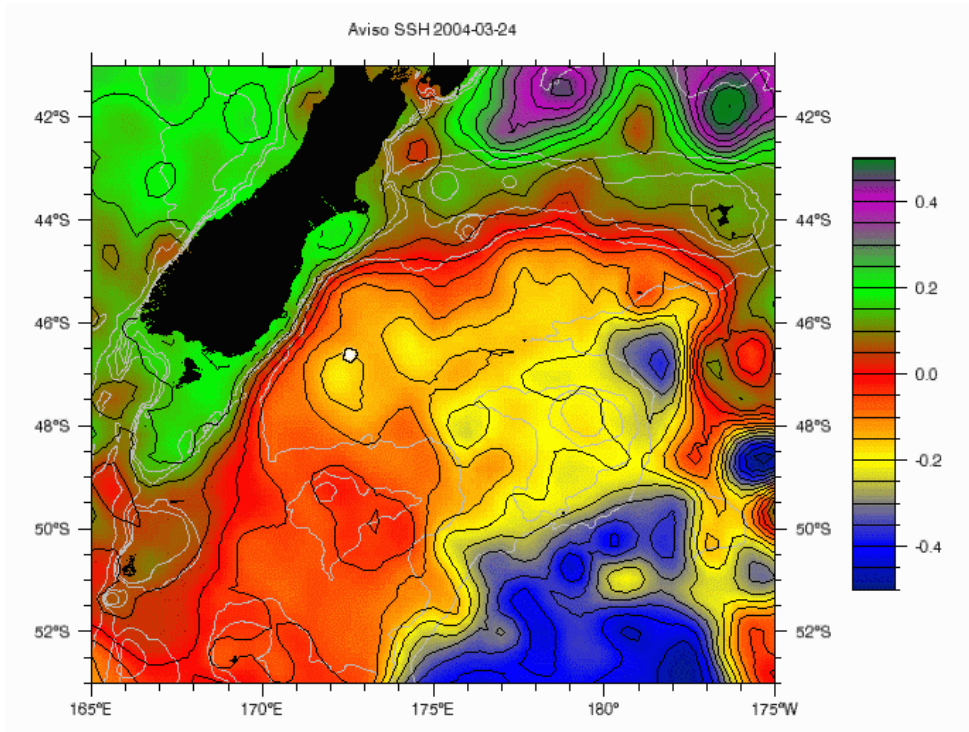


748
749
750
751
752
753

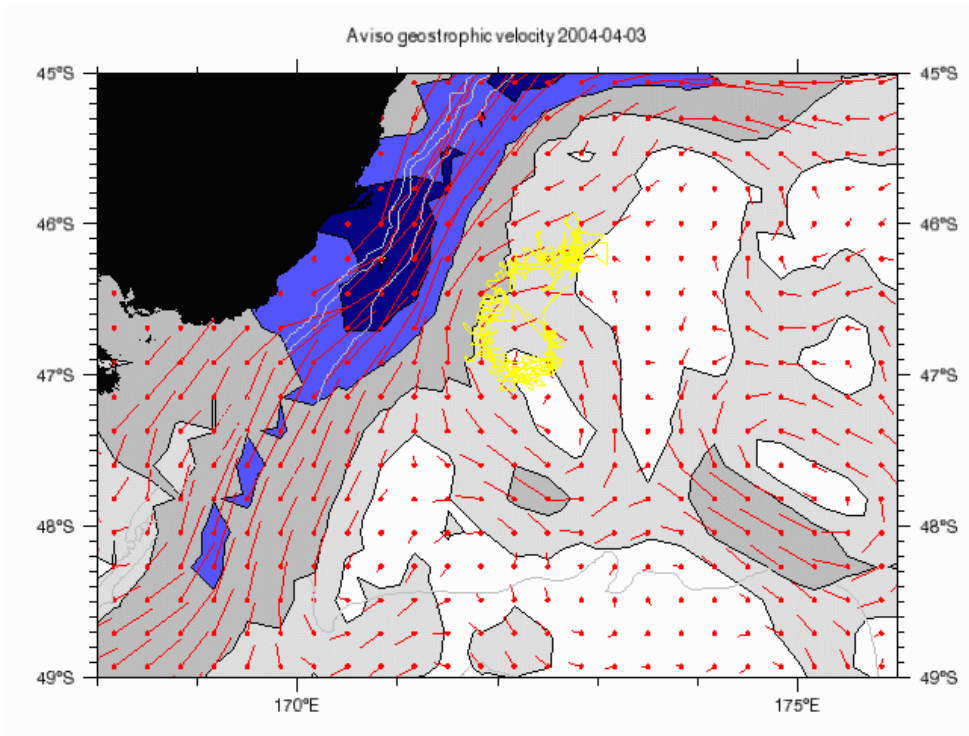
Figure 2: SeaWiFS chlorophyll-a composite Mar – Apr 2004 SAGE site is shown as a red dot.



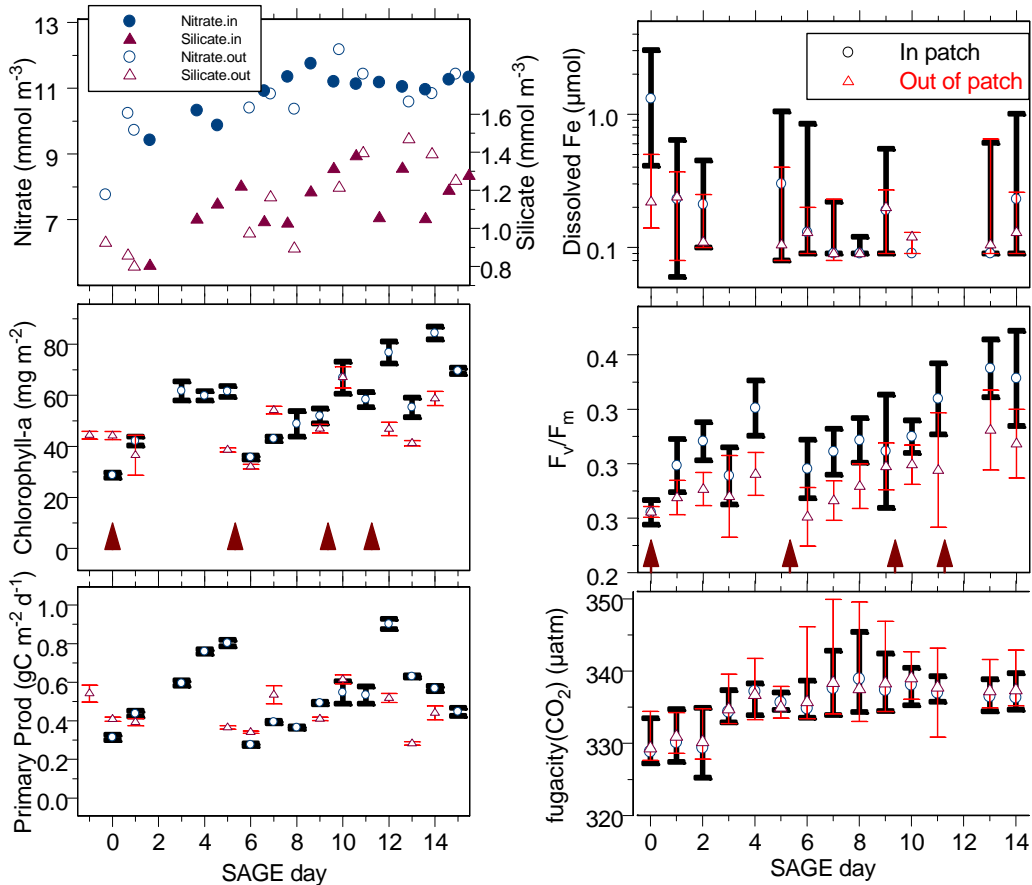
754
755 Figure 3: Timeline of SeaWiFS chlorophyll-a for SAGE site, extracted from 8 day composite
756 standard mapped images. Statistics are for a tile of up to 48 pixels (approx 50 x 50 km)
757 centred on 46.5°S 172.5°E. The vertical arrow marks the time of the SAGE experiment.
758
759



760
 761 Figure 4: Sea surface height plot for 24 March 2004 from AVISO delayed-time, reference,
 762 merged, Mapped Sea Level Anomalies (MSLA_DT_REF) from sea level anomaly data set at
 763 $0.25^\circ \times 0.25^\circ$ derived from satellite altimeters on TOPEX/Poseidon and ERS satellites
 764 www.aviso.oceanobs.com and NRL Coastal Ocean Model Sea Surface Height Mean. Release
 765 site is centred on the white dot. Anomaly (m) is indicated by the colour bar.
 766

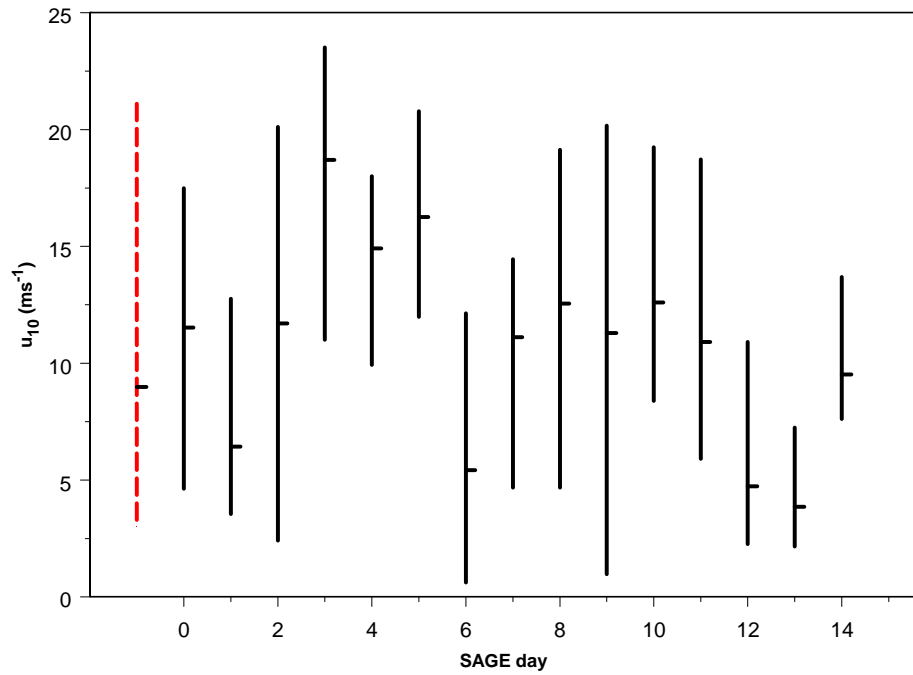


767
 768 Figure 5: Geostrophic current velocity calculated from SSH for 3 April 2004, data source as
 769 in Figure 4 (Hadfield, 2010). The yellow line shows the entire voyage track which
 770 progressed in an anti-clockwise direction. Current barbs show direction, filled contours show
 771 speed (m s^{-1}): 0–0.05 white, 0.05–0.10 light grey, 0.10–0.20 darker grey, 0.20–0.30 blue,
 772 0.30–0.40 navy.
 773

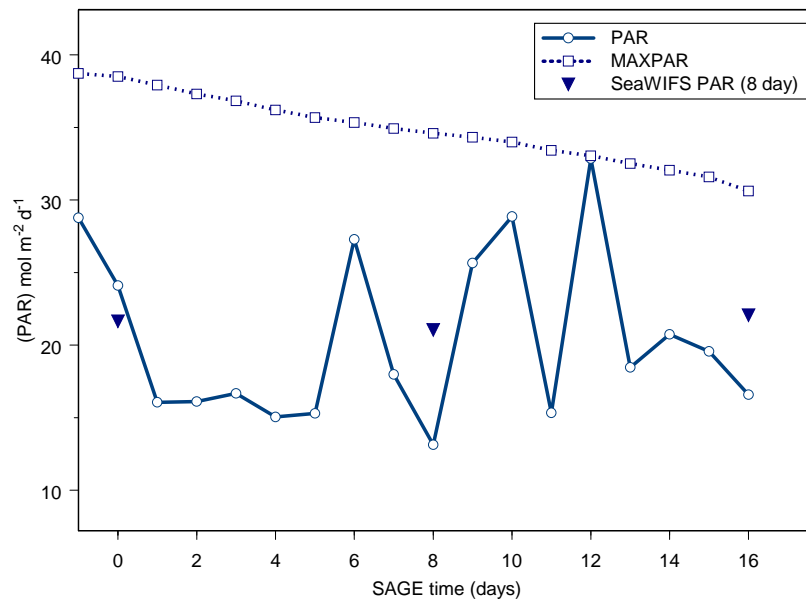


774
 775
 776
 777
 778
 779
 780
 781
 782
 783
 784
 785
 786
 787
 788
 789

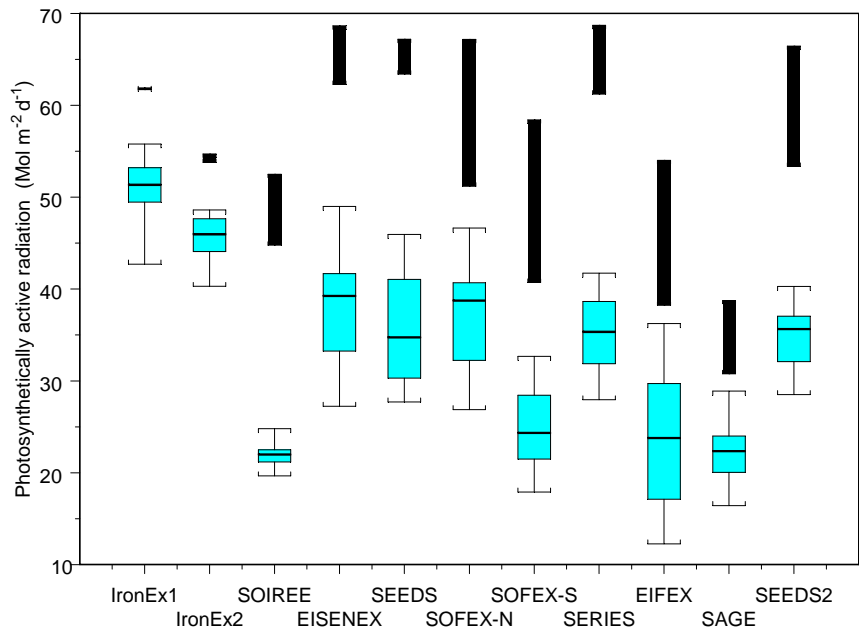
Figure 6: Evolution of the SAGE fertilised patch. Variables in the left column were measured from daily CTD casts, where Day 0 is the night 25/26 March (19:00 25-Mar-2004 for continuous data). The vertical arrows show the mid-times of the four iron infusions. Variables in the right column are from continuous underway seawater sampling where samples are assigned as in patch from SF₆ tracer levels above 10 fM and are otherwise regarded as OUT patch (a) Surface (top 10 m) nitrate and silicate concentrations IN and OUT of the patch. (b) Median surface (2 m) dissolved iron measured from towed torpedo trace iron sampler. The vertical bars extend between minimum and maximum values. (c) Total euphotic zone chlorophyll-*a* by trapezoidal integration to the 0.5 % light level as mean and standard error as calculated by Peloquin et al. (2010). (d) Photosynthetic competence F_v/F_m measured at night. Vertical bars show the mean and standard deviation for each night-time. (e) Total euphotic zone primary productivity by trapezoidal integration to the 0.5 % light level as mean and standard error as calculated by Peloquin et al. (2010). (f) Median fugacity of CO₂. The vertical bars extend between minimum and maximum values.



790
 791 Figure 7: Median, maximum and minimum daily u_{10} windspeed calculated from vessel
 792 anemometer and corrected for flow distortion according to Popinet et al. (2004). The dashed
 793 bar to the left shows a horizontal mark at the median and extends from the 5th to the 99th
 794 percentile of ship windspeed observations presented by Hadfield (2010)
 795
 796
 797

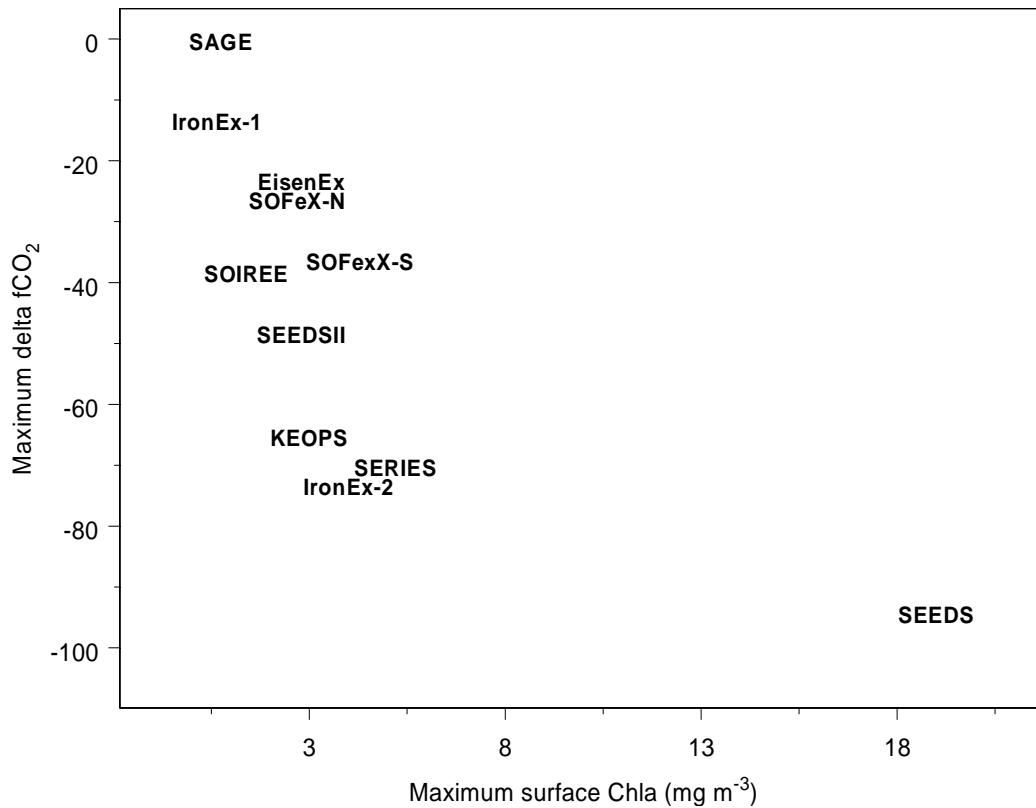


798
 799 ⁷ Figure 8: Measured and theoretical maximum clear sky daily incident photosynthetically
 800 active radiation calculated with an atmospheric transmission coefficient of 0.86 and top of the
 801 atmosphere PAR of 2500 $\mu\text{mol m}^{-2} \text{s}^{-1}$. Inverted triangles are 8-day composite surface PAR
 802 from SeaWIFS for $1^\circ \times 1^\circ$ box including the SAGE site presented by Hadfield (2010).
 803
 804



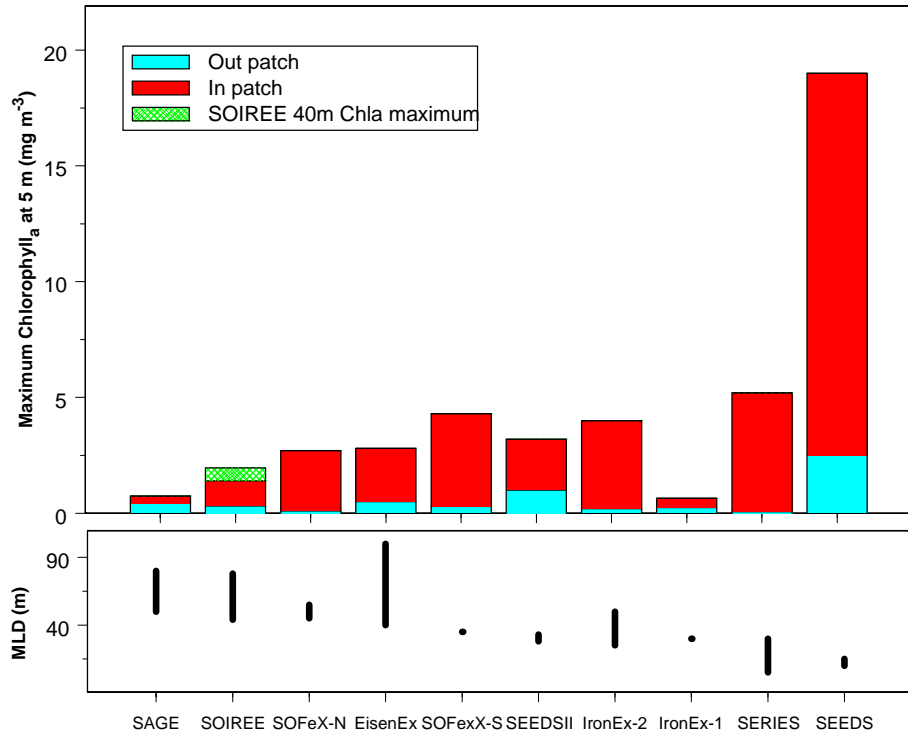
805
 806 Figure 9: Comparison of iron addition experiments. The black bars show the range of
 807 theoretical maximum clear sky daily incident PAR calculated with an atmospheric
 808 transmission coefficient of 0.86 and top of the atmosphere PAR of flux of $2500 \mu\text{mol m}^{-2} \text{s}^{-1}$.
 809 The blue box plots show the range, quartiles and median of surface PAR (allowing for
 810 cloudiness) based on 8-day composite SeaWiFS PAR (Frouin *et al.*, 2003) estimate for a 7×7
 811 tile of pixels at 9-km resolution over the duration of each experiment.

812
 813
 814



815
816
817
818
819
820
821
822

Figure 10: A comparison of the maximum in:out patch difference in fCO₂ versus the maximum surface chlorophyll for a number of FeAX's. Data sources are common with (Boyd et al., 2007) including supplemental tables. In addition SEEDS-II data were presented by (Tsumune et al., 2009); KEOPS are data from a study of natural iron fertilisation on the Kerguelen Plateau ((Blain et al., 2007).



823
 824 Figure 12: The enhancement in surface chlorophyll-*a* ranked in approximate order of
 825 reducing mixed-layer depth for 10 FeAX's (note IronEx-1 did not evolve due to subduction
 826 after 4 days).). Adapted from de Baar et al (2004), with inclusion of data from SEEDS II and
 827 SAGE (Boyd *et al.*, 2007 Suppl. tables)
 828
 829
 830